Synthesis of α-l-Araf and β-d-Galf series furanobiosides using mutants of a GH51 α-l-arabinofuranosidase

Jiao Zhao, Jérémy Esque, Isabelle André, Michael O'Donohue, Régis Fauré

Synthesis of α-L-Ara*f* and β-D-Gal*f* series furanobiosides using mutants of a GH51 α-L-arabinofuranosidase

Jiao Zhao, Jérémy Esque, Isabelle André, Michael J. O'Donohue*, Régis Fauré*

TBI, Université de Toulouse, CNRS, INRAE, INSA, Toulouse, France

* Corresponding authors.

E-mail addresses: michael.odonohue@inrae.fr (M.J. O'Donohue), regis.faure@insa-toulouse.fr (R. Fauré).

ABSTRACT

The GH-51 α-L-arabinofuranosidase from *Thermobacillus xylanilyticus* (*Tx*Abf) possesses versatile catalytic properties, displaying not only the ability to hydrolyze glycosidic linkages but also to synthesize furanobiosid -Ara*f* and β-D-Gal*f* series. Herein, mutants are investigated to evaluate their abil erform self-condensation, assessing both yield improvements and changes in regioselectivity. Overall yields of oligo-α-L-arabino- and oligo-β-D-galactofuranosides were increased up to 4.8-fold compared to the wild-type enzyme. In depth characterization revealed that the mutants exhibit increased transfer rates and thus a hydrolysis/self-condensation ratio in favor of synthesis. The consequence of the substitution N216W is the creation of an additional binding subsite that provides the basis for an alternative acceptor substrate binding mode. As a result, mutants bearing N216W synthesize not only (1,2)-linked furanobiosides, but also (1,3)- and even (1,5)-linked furanobiosides. Since the self-c sation is under kinetic control, the yield of homo-disaccharides was maximized using hi bstrate concentrations. In this way, the mutant R69H-N216W produced oligo-β-D-galactofuranosides in >70% yield. Overall, this study further demonstrates the potential usefulness of *Tx*Abf mutants for glycosynthesis and shows how these might be used to synthesize biologically-relevant glycoconjugates.

Keywords: biocatalysis, self-condensation, retaining glycoside hydrolase, furanobiosides, D-galactofuranosides, regioselectivity, acceptor binding subsites

Abbreviations: L-Ara*f*, α-L-arabinofuranosyl unit; α-L-Ara*f*O*p*NP, 4-nitrophenyl α-L-arabinofuranoside; D-Gal*f*, β-D-galactofuranosyl unit; β-D-Gal*f*O*p*NP, 4-nitrophenyl β-D-galactofuranoside; rGH, retaining glycoside hydrolase; *p*NP, 4-nitrophenol; SA, specific activity; *Tx*Abf, α-L-arabinofuranosidase from *Thermobacillus xylanilyticus*; T/H, transglycosylation/hydrolysis ratio.

1. Introduction

Furanoses are carbohydrates displaying a five-membered ring structure and are ubiquitous in Nature. An emblematic furanose is (2-deoxy-)D-ribofuranose, which forms an integral part of nucleic acids. Other furanoses are also widespread, with both L-arabinofuranose (L-Ara*f*) and its 5-hydroxymethyl analog D-galactofuranose (D-Gal*f*) frequently found in naturally occurring oligo- and polysaccharides, but absent in mammalian glyco-motifs [1–4]. L-Ara*f* moieties are mostly associated with cell wall, intercellular-matrix and extracellular structures (e.g. arabinoxylans [5,6], arabinogalactans [7] and arabinans [8,9]) in higher plant polysaccharides [6,8,9], while D-Gal*f* is widespread in glycoconjugates produced by pathogenic microorganisms [1,3,10]. Notably, the galactan portion of mycobacterial arabinogalactan is formed by a linear chain of alternating β-(1,5)- and β-(1,6)-linked D-Gal*f* residues [11]. Other glycomotifs, such as β-D-Gal*f*-(1,2)-β-D-Gal*f* are found in the mucins of the protozoan *Trypanosoma cruzi* [12] and β-(1,3)-linked D-Gal*f* moieties are present in oligosaccharidic structures of fungi [13–15] and bacteria [16].

Unsurprisingly, the widespread nature of L-Ara*f* and D-Gal*f* makes these two furanose forms interesting targets for synthetic chemistry. In the case of L-Ara*f*-containing compounds, these are of considerable interest for resea oses, particularly as substrates for plant cell wall acting enzymes [17]. Similarly, since rms part of antigenic epitopes in glycoconjugates of several pathogenic organisms, it constitutes a target for synthesis aimed at the development of diagnostic tools [18], or chemotherapeutic strategies [1].

In biological systems, furanose-containing carbohydrates are synthesized by arabino- and galactofuranosyltransferases, enzymes that use nucleotide sugar donors [18–21]. However, for *in vitro* synthesis, the use of these enzymes is challenging for a variety of reasons, despite recent progress in the field [22–25]. Similarly, the use of well-established synthetic chemistry strategi ught with difficulties, particularly because sugars in furanose configuration display less thermodynamic stability than their pyranose counterparts [26–28]. An alternative strategy to access furanose-bearing glycoconjugates is the use of transfuranosylases. Like glycosyltransferases, transfuranosylases are enzymes that possess the ability to synthesize furanose-containing compounds, using reactive furanosyl donor. However, unlike glycosyltransferases, transfuranosylases belong to the glycoside hydrolase (GH) class of enzymes and do not require the use of costly nucleotide sugars.

Transglycosylases are so-called retaining glycoside hydrolases (rGHs), meaning that these enzymes employ a double displacement mechanism to break down and synthesize glycosidic bonds [29]. In fact, transglycosylases are a specific subtype of rGHs that, while operating the same catalytic mechanism as hydrolytic rGHs, display strong propensity for transglycosylation, a reaction that involves the transfer of glycosyl donors onto glycoside acceptors. Regarding transfuranosylases, to our knowledge naturally-occurring examples are very rare, with transfructosylases being the most well-studied examples [30,31]. Nevertheless, hydrolytic α-L-arabinofuranosidases belonging to the GH51 family and possessing some ability to catalyze transarabinofuranosylation and transgalactofuranosylation have been described [2,32–36]. However, while α-L-arabinofuranosidases are relatively widespread and r s in the GH classification (GH43 and 51 are archetypal arabinofuranosidase families) [37], β-D-galactofuranosidases are rarer, with just a few examples being known to date [38,39]. In particular, using a large scale cloning, expression and screening approach, β-D-galactofuranosidases were recently revealed in GH5 and 43 families [40], but so far little biochemical characterization has been performed [41,42], thus it is too early to say whether these enzymes display significant ability to pe m transglycosylation reactions.

The GH51 α-L-arabinofuranosidase from *The cillus xylanilyticus* (*Tx*Abf) is a hydrolytic rGH that is active on substrates bearing α-L-Ara*f*-moieties (*e.g.* wheat, larchwood and oat spelt heteroxylans) [43]. Like other rGHs, *Tx*Abf hydrolyses glyosidic bonds using a two-step displacement mechanism that involves the formation of a transient covalent glycosyl-enzyme intermediate with the catalytic nucleophile residue [44]. Formation of this catalytic species is achieved through the glycosylation step. This involves binding of the donor substrate to the enzyme's active site and departure of donor leaving group, which is concomitantly protonated by a catalyti /base residue acting as a general acid. In the second so-called deglycosylation, step, the g zyme is usually broken down by a water molecule that displays nucleophilic character under the influence of a catalytic acid/base residue acting as a general base [29,32]. However, deglycosylation can also occur when other suitable incoming species adopt nucleophilic character. When deglycosylation is mediated by an incoming glycoside moiety, a new glycosidic bond is formed and the reaction is described as transglycosylation. Moreover, in the special case where the incoming acceptor species is the same as the donor species, the reaction is described as self-condensation.

Regarding *Tx*Abf, extensive studies have revealed that this enzyme is able to perform self-condensation using L-Ara*f*, D-Xyl*p* and D-Gal*f* as substrates, the latter reaching particularly

elevated yields [33,34]. Furthermore, *Tx*Abf has been the subject of protein engineering work aimed at improving its ability to perform transglycosylation [45–47]. However, so far no particular focus has been put on improving the self-condensation reactions performed by *Tx*Abf [33,34]. Previous work on self-condensation demonstrated that it was possible to synthesize α-L-arabino- and β-D-galacto-oligo-furanosides, but reported yields were modest and the regioselectivity of the reaction was mainly oriented towards the formation of (1,2)-linked regioisomers. While this regioselectivity might be useful for the synthesis of certain biologically-relevant α-L-arabino- and β-D-galactofurano-oligosaccharides, it is certainly not representative of the majority of medically-important glycoconjugates.

Herein, we focus on previously generated *Tx*Abf mutants [47,48], using these to evaluate their ability to perform self-condensation. In the course of this study we have carefully characterized regioselectivity in order to reveal the potentiality of the different *Tx*Abf mutants for use as synthetic tools to access a variety of α-L-arabinofurano- and β-D-galactofurano-containing oligosaccharides (Fig. 1).

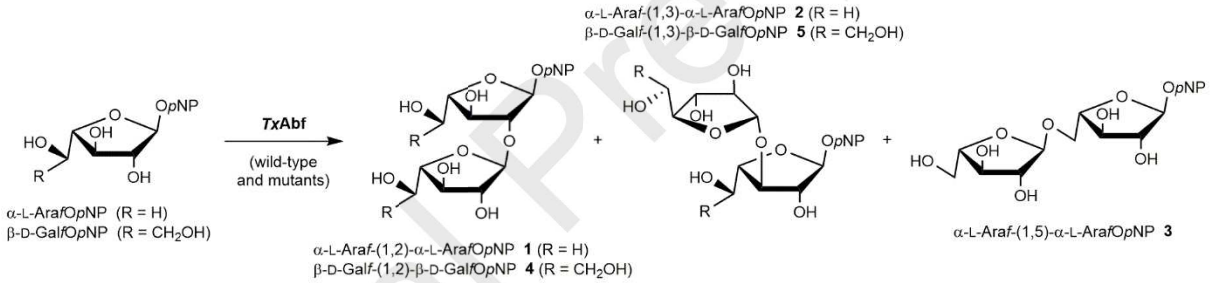

Fig. 1. Structures of the 4-nitrophenyl furanobiosides synthesized through self-condensation reactions catalyzed by *Tx*Abf and its mutants. Compounds **1**-**3** and **4**-**5** were products of self-condensation using α-L-Ara*f*O*p*NP and β-D-Gal*f*O*p*NP as substrate respectively. Stereochemistry at *C*-5 position is depicted for D-Gal*f* series (β-D-Gal*f*O*p*NP and compounds **4** and **5**, with R = CH_2OH).

2. Materials and methods

2.1. Substrates and chemicals

The substrates 4-nitrophenyl α-L-arabinofuranoside (α-L-Ara*f*O*p*NP) and 4-nitrophenyl β-D-galactofuranoside (β-D-Gal*f*O*p*NP) were obtained from CarboSynth. Molecular biology reagents were purchased from New England BioLabs.

130 *2.2. Mutagenesis, protein expression and purification*

131 *In vitro* site-directed mutagenesis was achieved using the QuikChange II Site-Directed
132 Mutagenesis Kit (Agilent). The plasmid pET24-*Tx*Abf (original pET vector was from Novagen)
133 containing the complete *Tx*Abf coding sequence (GenBank accession no CAA76421.2) was
134 used as the DNA template for mutagenesis. Mutations were introduced using a series of
135 oligonucleotide primers [48]. Mutagenesis, expression and purification of *Tx*Abf and mutants
136 thereof were performed as previously described [43,47,48]. Protein concentrations were
137 determined by measuring absorbance at 280 nm using a NanoDrop ND-2000 spectrophotometer.
138 Theoretical molecular weight and extinction coefficients were calculated using the ExPASy
139 ProtParam tool (https://web.expasy.org/protparam/).

140

141 *2.3. Enzymatic assay*

142 Enzyme activities were measured using a discontinuous assay [48]. Reactions were performed
143 in triplicate at 45 °C, using 5 mM β-D-Gal*f*O*p*NP as donor in 50 mM sodium phosphate buffer
144 at pH 7.0 with 1 mg·mL BSA, in a final reaction volume of 350 µL. Prior to enzyme addition,
145 reaction mixtures were pre-incubated at 45 °C. Once launched, reactions were conducted for
146 10-20 min, removing 40 µL samples at regular intervals. These samples were immediately
147 mixed with 200 µL of 1 M Na_2CO_3 and placed on ice. The release of 4-nitrophenol (*p*NP) was
148 monitored at 401 nm using a spectrophotometer (Infinite M200 Microplate reader, Tecan) and
149 quantified using an appropriate standard curve, prepared using pure *p*NP. Negative controls
150 containing all of the reactants except the enzyme were used to correct for spontaneous
151 hydrolysis of the donor substrate. Initial reaction rates were determined from the linear regions
152 of time-dependent plots, which correspond to less than 15% consumption of the donor substrate.
153 One unit (IU) of enzyme specific activity (SA) corresponds to the amount of enzyme releasing
154 one µmol of *p*NP per minute. The kinetic parameters K_M, k_{cat} and k_{cat}/K_M were determined by
155 measuring enzyme SA at various substrate concentrations. The β-D-Gal*f*O*p*NP was varied from
156 0.2-30 mM. A modified version of Michaelis-Menten equation (Table 2) was applied to fit the
157 nonlinear regression plot of SA versus [S] (substrate concentration) using SigmaPlot 11.0
158 software.

159

160

161

2.4. NMR analysis

To monitor reactions, ^{1}H NMR spectra were collected using a Bruker Avance II spectrometer equipped with a TCI probe and operating at 500 MHz. Reactions were performed at 45 °C with α-L-Ara*f*O*p*NP or β-D-Gal*f*O*p*NP containing appropriately diluted enzymes in a total volume of 600 µL (containing 10% D_2O in 10 mM sodium phosphate buffer at pH 7.0, v/v; with 1 $mg \cdot mL^{-1}$ BSA). To initiate reactions, a fixed (10% of total reaction volume) aliquot of enzyme solution was added, with the enzyme concentration being chosen to reach maximal transglycosylation yield within a timeframe that was similar for all reactions. In the α-L-Ara*f*O*p*NP self-condensation reaction, 0.003 µM wild-type *Tx*Abf, 0.27 µM R69H-N216W, 0.45 µM R69H-N216W-L352M and 1.01 µM F26L-R69H-N216W were used while, in the β-D-Gal*f*O*p*NP self-condensation reaction, 0.27 µM wild-type *Tx*Abf, 4.00 µM R69H-N216W and 41.80 µM R69H-N216W-L352M were used. Time course NMR monitoring was achieved by performing pseudo-2D kinetics experiments based on a phase sensitive NOESY sequence with pre-saturation, with spectra being accumulated every 8.7 min (2 × 32 scans). Using previously determined SAs, it was possible to adjust enzyme quantities to suit a 18-h reaction time frame, although the actual duration of the reaction was dependent on the enzyme used. The pH in 10% D_2O was measured using a glass pH electrode, applying the modified equation $pH_{10\%\ D_2O} = pH_{electrode} + 0.04$ [49]. The chemical shift reference was based on the HOD signal calibrated at 4.55 ppm at 45 °C [50].

Donor (*i.e. p*NP-glycofuranoside) consumption and the apparition of self-condensation furanobiosides **1-5** were quantified by integrating the anomeric proton signals from the *p*NP-linked furanosyl moiety (H-1a). For self-condensation products, the blinded anomeric protons associated with the non-reducing end of the furanosyl unit (H-1b) were not taken into account, because they overlap with the anomeric protons of the monosaccharide hydrolysis product. The selected anomeric protons and their chemical shifts are shown in Table 1. Donor substrate was qu ied by integrating its relevant anomeric proton signals (Fig. 1 and Supplementary Figs. S !). The molarity of all compounds was normalized relative to the initial proton integral of the donor compound. Yields of self-condensation products were maximal yields expressed as a percentage of initial donor concentration. The mean value of the *ortho* and *meta* protons of the linked *p*NP were regarded as the sum of the donor and self-condensation products. Thereby, the overall yield of self-condensation products was calculated by subtracting the value of the integral of the anomeric donor signal from half the value of the average integral of *ortho* and

194 *meta* aromatic protons of the linked *p*NP signals (Supplementary Fig. S3). In doing so, we were
195 able to account even for minor products, which taken alone were barely detectable.

196

197 **Table 1**

198 Chemical shift of the substrates and self-condensation products **1-5** (Fig. 1) used for quantifying
199 the evolution of enzymatic reaction.[a]

Compound	δ (ppm)	
	H-1a	Aromatic H_m and H_o of *p*NP moiety
α-L-Ara*f*O*p*NP	5.78	8.20-8.18 and 7.18-7.16
1 α-L-(1,2)	5.89	
2 α-L-(1,3)	5.81	
3 α-L-(1,5)	5.79	
β-D-Gal*f*O*p*NP	5.74	8.20-8.18 and 7.18-7.16
4 β-D-(1,2)	5.82	
5 β-D-(1,3)	5.78	

200 [a] The chemical shifts were analyzed at 45 °C and pH 7 in buffered 10% D_2O. Chemical shifts
201 of self-condensation furanobiosides **1-5** were referred to previous work [2,33,34,48].

202

203 *2.4. Modelling* Tx*Abf and R69H-N216W-L352M in complex with self-condensation products*

204 Crystallographic data of the inactive *Tx*Abf E176Q (PDB: 2VRQ) and the mutant R69H-
205 N216W-L352M (PDB: 6ZT8) [48], were used to construct a complete 3D model of the mutant
206 R69H-N216W-L352M. Next, α-L-Ara*f* disaccharides (without *p*NP) were built using Glycam
207 Force Field and tleap program from AMBER16 software suite [51]. For each α-L-Ara*f*
208 disaccharide, a short minimization in implicit solvent (Generalized Born) with 250 steps of
209 steepest descent and 250 steps of conjugated gradient was performed, using a cut-off of 99 Å.
210 *p*NP aglycon was added at the reducing end and geometrically optimized using Avogadro
211 software [52]. β-D-Gal*f* disaccharide structures were derived from the corresponding α-L-Ara*f*
212 disaccharides by adding hydroxymethyl on each α-L-Ara*f* unit using Avogadro software. The
213 complexes formed by the enzyme and the self-condensation products (**1-5**) were initially
214 assembled in PyMol [53] by pair fitting onto bound α-L-Ara*f* (occupying subsite -1) in X-ray
215 structure of the inactive *Tx*Abf E176Q (PDB: 2VRQ). Complexes were further subjected to
216 energy minimization macro supplied in the YASARA package (version 12.8.1) [54], using

AMBER and GAFF Force Fields for the protein and the ligand, respectively. The figure was then prepared using PyMol Molecular Graphics System, v0.99 (Schrödinger).

3. Results

3.1. Kinetic analysis of Tx*Abf mutants*

Measurement of steady state kinetic parameters of α-L-Ara*f*O*p*NP conversion (monitoring *p*NP release) catalyzed by *Tx*Abf and its mutants revealed that all mutations severely affected catalytic efficiency (Table 2). This was also the case for *Tx*Abf acting on β-D-Gal*f*O*p*NP. The values were reduced by more than two and three orders of magnitude in reactions containing α-L-Ara*f*O*p*NP and β-D-Gal*f*O*p*NP respectively. Comparing the k_{cat}/K_M values of reactions catalyzed by the wild-type enzyme acting on either of the two substrates (α-L-Ara*f*O*p*NP and β-D-Gal*f*O*p*NP) revealed a more than 6 000-fold difference. Regarding the reaction involving α-L-Ara*f*O*p*NP and R69H-N216W-L352M the K_M value was relatively similar to that of the reaction catalyzed by the wild-type enzyme, whereas the same reaction catalyzed by F26L-R69H-N216W is characterized by significant decreases in both k_{cat} and K_M. Assuming that deglycosylation is rate-limiting, the lowered k_{cat} value leads us to postulate that R69H-N216W-L352M is mostly impaired with respect to deglycosylation, whereas the impact of F26L-R69H-N216W appears to be more complex, affecting both steps [47]. Regarding the reaction involving R69H-N216W and β-D-Gal*f*O*p*NP, a two-phase reaction profile was observed that did not reach saturation (Fig. 2) [47,48]. Remarkably, unlike wild-type *Tx*Abf, the mutant R69H-N216W yielded a measurable K_M value (0.45 mM) for the reaction containing β-D-Gal*f*O*p*NP, which is in the same order of magnitude to that of wild-type *Tx*Abf acting on α-L-Ara*f*O*p*NP (0.25 mM). Nevertheless, because the k_{cat} value of the reaction is also extremely low, the overall catalytic efficiency of R69H-N216W acting on β-D-Gal*f*O*p*NP is unchanged compared to the reaction involving wild-type *Tx*Abf.

Table 2

Kinetic parameters of reactions catalyzed by *Tx*Abf and mutants thereof, using α-L-Ara*f*O*p*NP or β-D-Gal*f*O*p*NP as substrate.

Enzyme	SA_{th} (IU·mg^{-1})	K_M (mM)	k_{cat} (s^{-1})	k_{cat}/K_M (s^{-1}·mM^{-1})	N_S[a] (s^{-1}·mM^{-1})
α-L-Ara*f*O*p*NP					
*Tx*Abf[b]	615	0.72	575	795	-
*Tx*Abf[c]	145	0.25	139	556	-
R69H-N216W-L352M[c]	0.60	0.48	0.58	1.21	0.034
F26L-R69H-N216W[c]	0.16	0.01	0.15	10.81	0.034
β-D-Gal*f*O*p*NP					
*Tx*Abf[b]	15.6	>50[d]	15.02	0.13	-
R69H-N216W[e]	0.065	0.45	0.06	0.14	0.008

[a] Ns is a nonspecific constant that is included in the modified Michaelis-Menten equation to account for activation of the enzyme by the self-condensation product: $SA_{app.} = SA_{th.}\cdot[S]/(K_M + [S]) + N_S\cdot[S]$ where $SA_{th.}$ is the theoretical maximum activity achieved if the enzyme operates according to the Michaelis-Menten model.

[b] The kinetic parameters were referred to previous work at 60 °C in 50 mM sodium acetate buffer pH 5.8 [55,56].

[c] The kinetic parameters were referred to previous work at 45 °C in 50 mM sodium phosphate buffer pH 7. [48]

[d] The K_M v estimate, because its measurement was unfeasible due to the limited solubility of the substrate.

[e] Kinetic assays were carried out in triplicate at 45 °C in 50 mM sodium phosphate buffer pH 7.0. Relative errors were inferior to 10%.

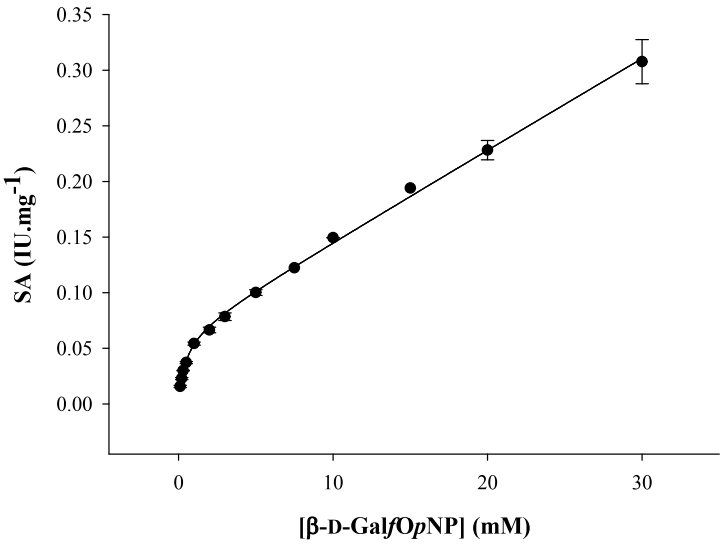

Fig. 2. Specific activity (SA) as a function of β-D-Gal*f*O*p*NP concentration for R69H-N216W.

*3.2. Self-condensation profile using α-L-Araf*O*pNP as donor*

When using *Tx*Abf, the yield of the major self-condensation product **1**, α-L-Ara*f*-(1,2)-α-L-Ara*f*O*p*NP (Fig. 1 and Table 3), is consistent with that previously reported [34]. This compound was accompanied by trace amounts of compounds **2** and **3**, corresponding to (1,3) and (1,5) linkages respectively. Compared to *Tx*Abf, the three R69H-N216W-containing mutants exhibited enhanced ability to p elf-condensation, with overall yields being 3.5- to 3.8-fold higher. Moreover, increased yield was coupled to significant changes in enzyme regioselectivity, with the proportion (% of total yield) of (1,3)-linked product **2** increasing from 30% (*Tx*Abf) to >70% in reactions catalyzed by the mutants, and even reaching 82% in the case of R69H-N216W. Overall, the three mutants were similar in terms of both regioselectivity and yields.

Using real time NMR spectroscopy (Supplementary Fig. S1), it was possible to monitor the evolution of each self-condensation product, and thus observe secondary hydrolysis during the latter stages of the reaction. For wild-type *Tx*Abf (Fig. 3A and Supplementary Fig. S4A), the maximum yield (7%) of the major product **1** was reached at 68% conversion of α-L-Ara*f*O*p*NP, meaning that hydrolysis was the predominant reaction. Concerning the R69H-N216W-containing mutants, maximal yields were achieved at later stages in the reaction, when the conversion of α-L-Ara*f*O*p*NP was higher, *i.e.* 88, 90 and 92% for F26L-R69H-N216W, R69H-N216W and R69H-N216W-L352M respectively (Fig. 3B-D and and Supplementary Fig. S4B-D). This means that compared to wild-type *Tx*Abf, secondary hydrolysis was delayed in

reactions catalyzed by the mutants. When comparing the decomposition rate of major compound **2**, it is clear that R69H-N216W performs secondary hydrolysis (v_{HII}) at a higher rate than R69H-N216W-L352M and F26L-R69H-N216W (Supplementary Table S1). Additionaly, the overall self-condensation yield of this double mutant is slightly lower than that of the other two mutants. However, as a synthetic tool, R69H-N216W can be considerd the best all-round performer. This conclusion is based on its combined performance: yield of the major product **2**, synthesis rate v_S and SA (Table 3 and Supplementary Table S1). Finally, R69H-N216W-L352M displayed the highest self-condensation/secondary hydrolysis (v_S/v_{HII}) ratio with a value of 3.0 (Supplementary Table S1).

Table 3

Maximal self-condensation yields (in %) using α-L-Ara*f*O*p*NP as donor.

Enzyme	SA (IU·mg^{-1})[a]	**1** α-L-(1,2)	**2** α-L-(1,3)	**3**[b] α-L-(1,5)	Overall yield[c]
*Tx*Abf	261.79 ± 10.72	7	3	2	10
R69H-N216W	1.60 ± 0.02	6	37	8 (3)	45
R69H-N216W-L352M	0.97 ± 0.11	10	34	6 (3)	47
F26L-R69H-N216W	0.32 ± 0.01	6	38	8 (4)	48

[a] Specific activities (SA) referred to previous work at 45 °C in 50 mM sodium phosphate buffer pH 7.0 containing 5 mM α-L-Ara*f*O*p*NP and were measured by monitoring *p*NP release using a discontinuous assay.

[b] Since maximal yield of product **3** was reached later than those of products **1** and **2**, the yield of **3** when **1** and **2** are maximum is shown in brackets.

[c] Maximal yields of each disaccharide are reached after different incubation times. This explains why overall yields are not equal to the sum of the maximum yield of each disaccharide.

In absolute terms, the yield of α-L-Ara*f*-(1,5)-α-L-Ara*f*O*p*NP **3** was also slightly (3- or 4-fold) increased in reactions catalyzed by the mutants. However, in relative terms the proportion of compound **3** was slightly reduced from 20% of total yield (*Tx*Abf) to as little as 6% (R69H-N216W-L352M) when maximal total transglycosylation yield was reached. Significantly, although the yield of compound **3** is low for the mutants, it continues to be produced, even when α-L-Ara*f*O*p*NP is consumed (Fig. 3B-D). This observation suggests that at later stages in the

reaction, compound **3** is formed via hydrolysis of compounds **1** and **2** and the rate of hydrolysis of compound **3** is inferior to that of its synthesis.

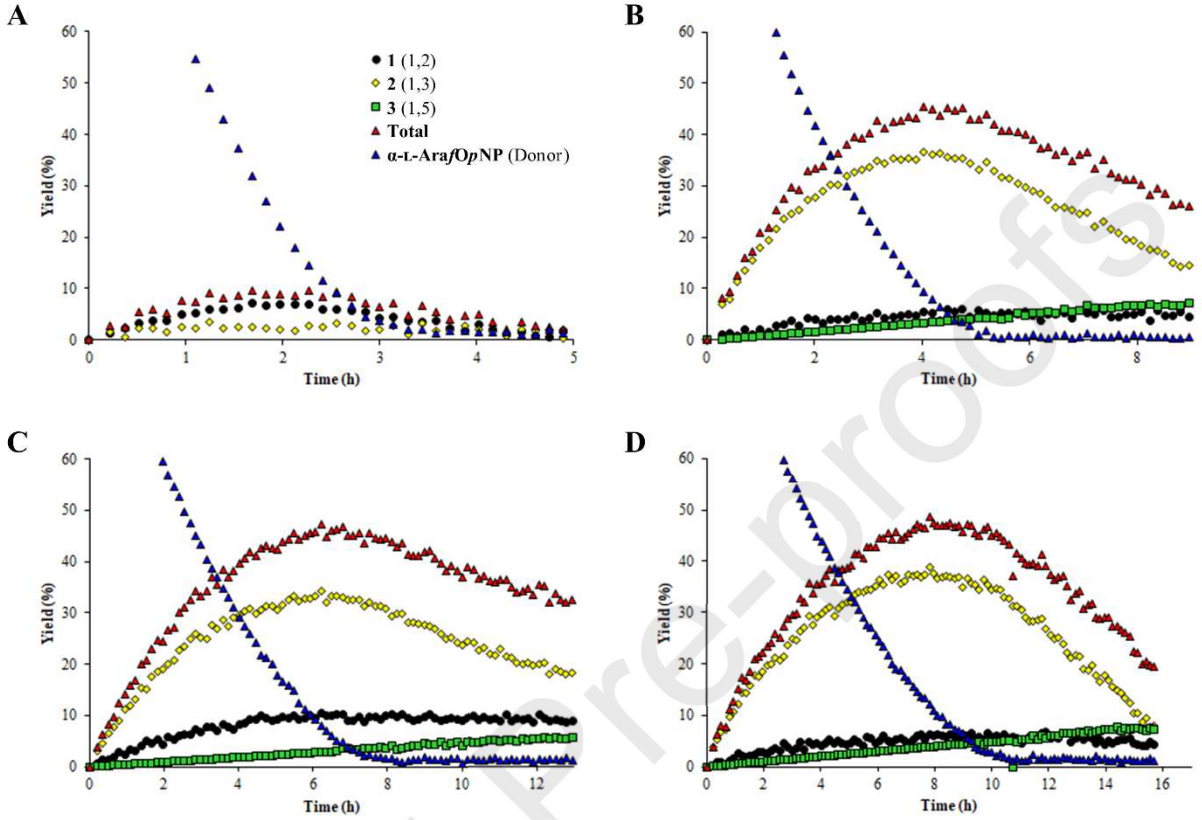

Fig. 3. Monitoring of α-L-Ara*f*O*p*NP consumption and the apparition of the different self-condensation products **1**-**3** as a function of time in reactions catalyzed by (A) *Tx*Abf, (B) R69H-N216W, (C) R69H-N216W-L352M, and (D) F26L-R69H-N216W.

*3.3. Self-condensation profile using β-D-Gal*f*O*p*NP as donor*

Despite being a poor substrate for *Tx*Abf-mediated hydrolysis, β-D-Gal*f*O*p*NP readily participated in the self-condensation reaction (Fig. 1), procuring a 24% overall yield of oligosaccharide products (Table 4). The major product **4**, β-D-Gal*f*-(1,2)-β-D-Gal*f*O*p*NP (18% yield), represents 75% of the regioisomeric mixture, revealing the good regioselectivity of wild-type *Tx*Abf in this reaction. This observation is highly consistent with previous work performed both on *Tx*Abf [33] and other GH51 Abf [2] and further confirms the natural propensity of the wild-type enzyme to hydrolyze and synthesize (1,2)-linkages. Characterization of mutants containing single substitutions (R69H and N216W) revealed that these display regioselectivities and yields similar to those of *Tx*Abf (Table 4, Fig. 4A and Supplementary Fig.

S5). However, combination of these point mutations (*i.e.* R69H-N216W and R69H-N216W-L352M) yielded enzymes that double the total product yield and procure regioisomeric mixtures containing a (1,3)-linked disaccharide **5** at a yield of 18 (R69H-N216W-L352M) and 22% (R69H-N216W) respectively. In this respect, the yield of product **4** was relatively unaltered, meaning that the gains in overall yield can be completely attributed to the vast improvement in the enzyme's ability to form regioisomer **5** (Table 4 and Supplementary Fig. S2).

Table 4

Maximal self-condensation yields (in %) using β-D-Gal*f*O*p*NP as donor.

Enzyme	SA (IU·mg^{-1})[a]	**4** β-D-(1,2)	**5** β-D-(1,3)	Overall yield[b]
*Tx*Abf	1.23 ± 0.09	18	2	24
R69H	0.05 ± 0.0003	18	3	24
N216W	1.33 ± 0.035	21	3	24
R69H-N216W	0.09 ± 0.001	15	22	47
R69H-N216W-L352M	0.025 ± 0.001	16	18	45

[a] SA was measured by monitoring *p*NP release using a discontinuous assay. Assays were carried out at 45 °C in 50 mM sodium phosphate buffer pH 7.0 using 5 mM β-D-Gal*f*O*p*NP.

[b] Overall yield is higher than the sum of compound **4** and **5** due to the presence of small amounts of β-D-(1,5) and β-D-(1,6)-linked disaccharides and traces of *p*NP oligo-β-D-galactofuranosides displaying degrees of polymerization >2.

In reactions catalyzed by wild-type *Tx*Abf, the maximum yield of galactofuranobiosides **4** and **5** was reached when 70% of the substrate had been consumed. However, in the case of the mutants, this point was shifted to 92 (R69H-N216W-L352M) and 96% (R69H-N216W) respectively. Despite this difference between reactions catalyzed by wild-type and mutant enzymes, it is noteworthy that in all three cases the self-condensation products displayed remarkable stability, meaning that secondary hydrolysis was strongly diminished, even at very low donor substrate concentrations (Fig. 4B-C). This was particularly noticeable for the reaction involving the mutant R69H-N216W (Fig. 4B and Supplementary Fig. S6), since product decomposition was barely perceptible. Therefore, accounting for the additional fact that R69H-

N216W displayed 3.6-fold higher catalytic activity than the triple mutant (Table 4), this enzyme can be regarded as the best performing enzyme in terms of β-D-Gal*f*O*p*NP self-condensation.

Although the major products of α-L-Ara*f*O*p*NP and β-D-Gal*f*O*p*NP self-condensation were disaccharides, in reactions catalyzed by *Tx*Abf enzymes (more for the mutants), trisaccharides were also observed. However, due to the small quantity produced and the fact that NMR signals overlapped with those of the disaccharides, these trisaccharides were neither quantified, nor fully characterized. Nevertheless, their detection further demonstrates the aptitude of the mutant enzymes to synthesize L-Ara*f* and D-Gal*f*-oligosaccharides.

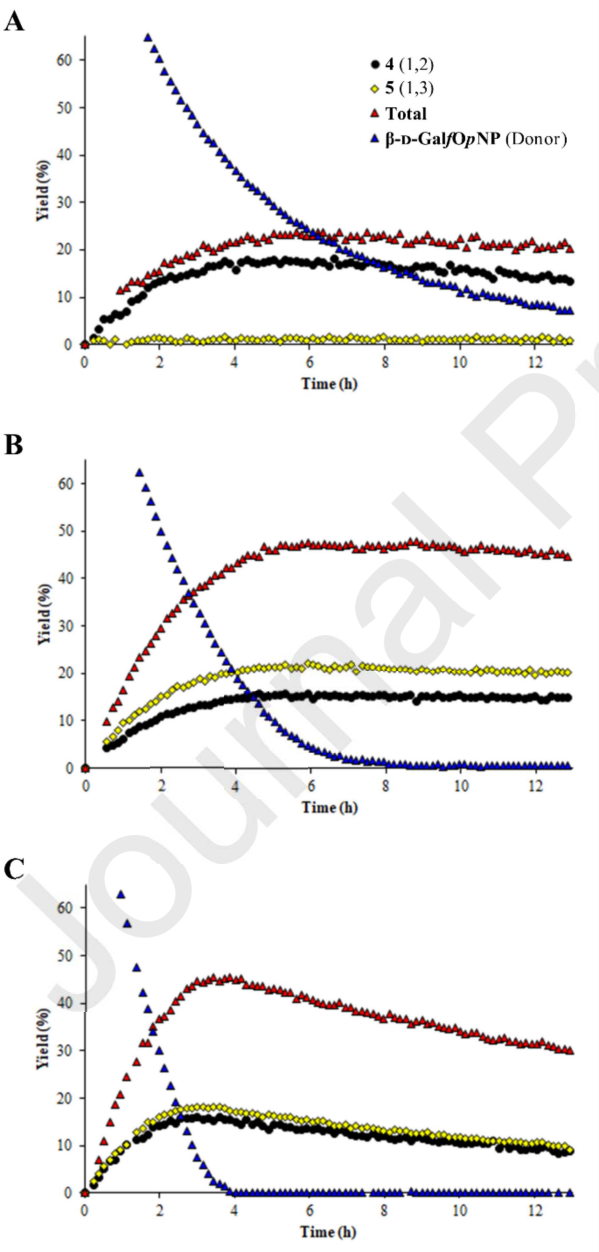

Fig. 4. Monitoring of β-D-Gal*f*O*p*NP consumption and the apparition of the different self-condensation products **4-5** as a function of time in reactions catalyzed by (A) *Tx*Abf, (B) R69H-N216W, and (C) R69H-N216W-L352M.

3.4. Probing the relationship between substrate concentration and global synthesis yield

In view of the catalytic superiority of R69H-N216W for the self-condensation of β-D-Gal*f*O*p*NP, this enzyme was employed to explore how substrate concentration influences the global yield of products (Fig. 5). Increasing substrate concentration clearly elevated both total self-condensation yield and the rate of donor conversion into self-condensation products (Fig. S6). Moreover, increasing β-D-Gal*f*O*p*NP concentration delayed the (tipping) point at which secondary hydrolysis became dominant, outweighing self-condensation. Consequently, the linear phase of self-condensation of the R69H-N216W-catalyzed reactions was extended at higher substrate concentration, meaning that the reaction is mainly under kinetic control. An overall yield of 72% was achieved when using 30 mM of β-D-Gal*f*O*p*NP. Considering substrate solubility, this is close to the maximum achievable yield in an aqueous reaction system.

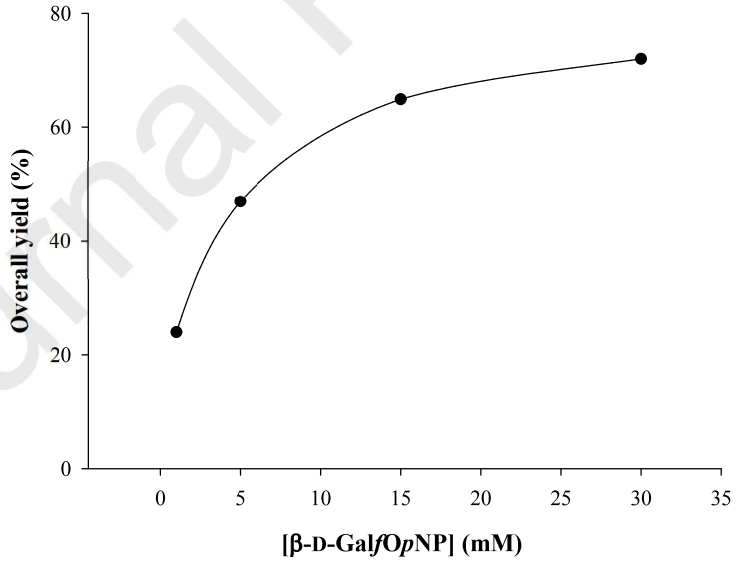

Fig. 5. Relationship between β-D-Gal*f*O*p*NP substrate concentration and overall self-condensation yield in the R69H-N216W-catalyzed reaction.

3.5. Getting molecular insight on the regioselectivity of the mutant enzymes

To investigate the regioselectivity of the mutant enzymes, 3D models of *Tx*Abf and R69H-N216W-L352M complexed to self-condensation products **1-5** were built (Fig. 6). Strikingly, analysis of the models reveals that mutation of Asn216 by a tryptophan residue (N216W) engenders cleft topology better-adapted for binding to the more linear (1,3)-linked furanobiosides. The presence of tryptophan provides a putative stacking interaction with *p*NP group. This observation is fully consistent with the experimental results associated with both the double and triple mutants. Moreover, 3D models suggest that the nature of the furanosyl moieties (L-Ara*f* *vs* D-Gal*f*) does not significantly alter product positioning and binding interactions in the active site, consistent with the fact that the impact of N216W on regioselectivity is equivalent when either α-L-Ara*f*O*p*NP or β-D-Gal*f*O*p*NP are used as substrates. Comparing binding of the (1,2)- and (1,3)-linked compounds, occupation of subsite -1 is globally very similar, probably because the spatial confinement of this pocket-like subsite, combined with a significant number of specific enzyme-substrate interactions therein does not provide room for alternative binding modes [57]. However, some differences are observed in subsite +1 depending on the nature of the furanosyl moiety occupying the site and on how the *p*NP moiety is accommodated (Fig. 6). In the case of (1,2)-linked compounds, 3D models suggest that both the wild-type and mutant enzymes accommodate the *p*NP moiety in subsite +2 [57], which contains residue Trp302, likely establishing a π-π stacking interaction (distances < 3.8 Å) with the *p*NP moiety (Fig. 6A, C, E and G). Regarding (1,3)-linked products, the model reveals that the *p*NP moiety lies in a different spatial position and thus occupies an alternative subsite, designated here as +2''. In the wild-type enzyme, subsite +2'' contains Asn216 (Fig. 6B and F), where this residue is substituted by a tryptophan in the mutant enzymes. This forms a novel hydrophobic platform, favorable for a π-π interaction (distances < 4.1 Å) with the *p*NP moiety (Fig. 6D and H). Consequently, this modification putatively creates a new binding mode for (1,3)-linked furanobiosides that is absent in wild-type *Tx*Abf. It is noteworthy that the emergence of an alternative subsite +2'' in the mutant enzymes does not alter subsite +2, which explains why the mutants do not lose their ability to form (1,2)-linked self-condensation products. Indeed, the initial interactions of *p*NP from compound **1** and **4** with Trp 248, Trp302 and putatively Lys251 are retained for R69H-N216W-L352M (Supplementary Fig. S7).

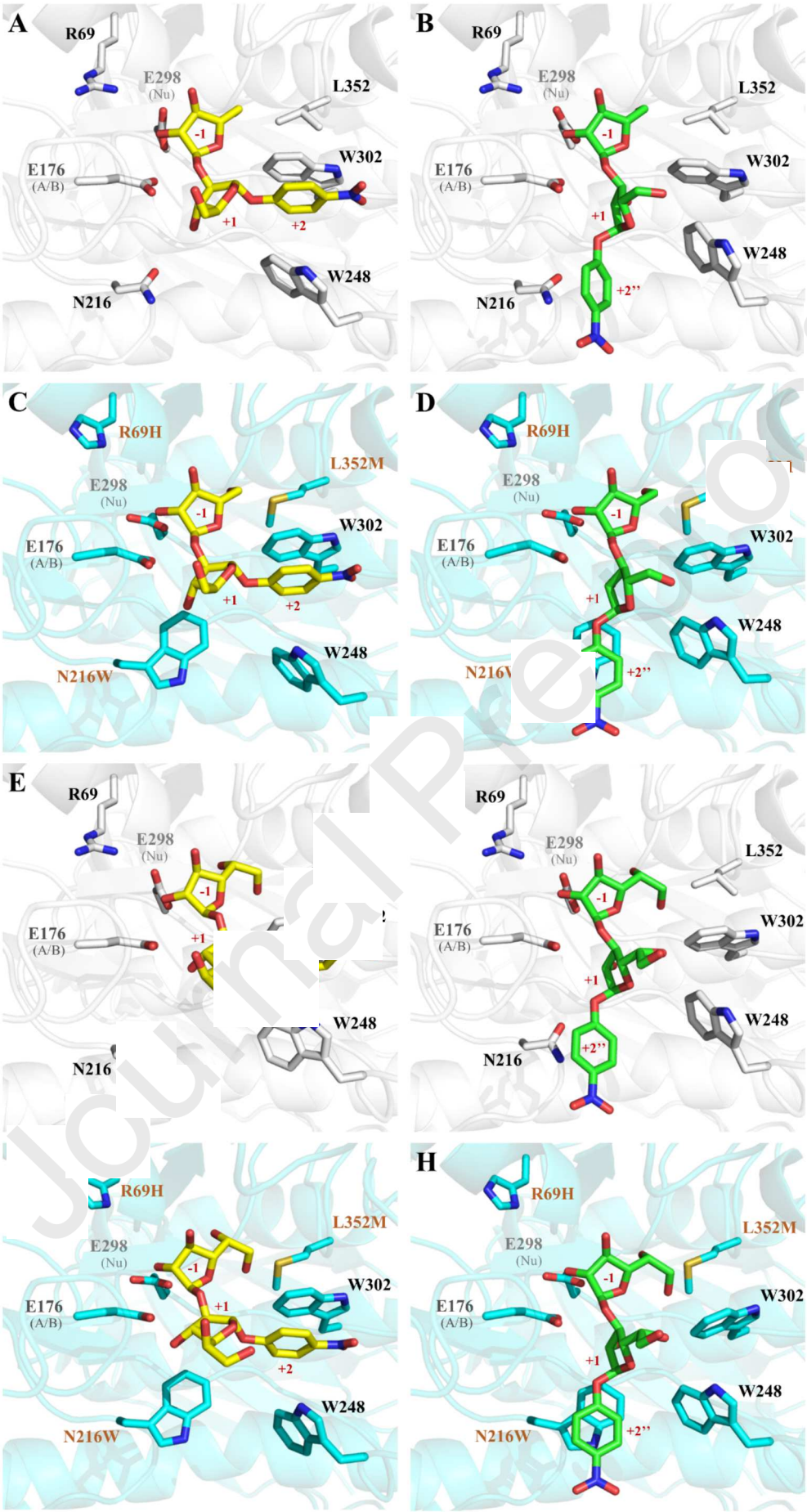
A
R69
E298
(Nu)
L352
-1
W302
E176
(A/B)
+1
+2
W248
N216
B
R69
E298
(Nu)
L352
-1
W302
E176
(A/B)
+1
W248
+2''
N216
C
R69H
L352M
E298
(Nu)
-1
W302
E176
(A/B)
+1
+2
W248
N216W
D
R69H
E298
(Nu)
-1
W302
E176
(A/B)
+1
W248
N216
+2''
E
R69
E298
(Nu)
-1
E176
(A/B)
+1
W248
N216
R69
E298
(Nu)
L352
-1
W302
E176
(A/B)
+1
W248
+2''
N216
R69H
L352M
E298
(Nu)
-1
W302
E176
(A/B)
+1
+2
W248
N216W
H
R69H
L352M
E298
(Nu)
-1
W302
E176
(A/B)
+1
W248
N216W
+2''

418

Fig. 6. Wild-type *Tx*Abf (grey) and R69H-N216W-L352M (cyan) bound to products **1** or **4** (yellow) and **2** or **5** (green): (A**)** *Tx*Abf bound to its major product **1**, α-L-Ara*f*-(1,2)-α-L-Ara*f*O*p*NP; (B) *Tx*Abf bound to its minor product **2**; (C) R69H-N216W-L352M bound to its minor product **1**; (D) R69H-N216W-L352M bound to its major product **2**, α-L-Ara*f*-(1,3)-α-L-Ara*f*O*p*NP; (E) *Tx*Abf bound to its major product **4**, β-D-Gal*f*-(1,2)-β-D-Gal*f*O*p*NP; (F) *Tx*Abf bound to its minor product **5**; (G) R69H-N216W-L352M bound to its minor product **4**; and (H) R69H-N216W-L352M bound to its major product **5**, β-D-Gal*f*-(1,3)-β-D-Gal*f*O*p*NP. The protein is shown in cartoon, whereas the key labelled residues and the ligands are shown in stick representation. Mutations and subsites are labelled (brown and red characters respectively).

Finally, experimental data revealed that, in the presence of α-L-Ara*f*O*p*NP, mutant enzymes displayed greater ability to produce (1,5)-linked products. 3D modelling of α-L-Ara*f*-(1,5)-α-L-Ara*f*O*p*NP **3** shows that this disaccharide adopts a conformation that is similar (albeit more extended) to that of α-L-Ara*f*-(1,3)-α-L-Ara*f*O*p*NP **2**. Accordingly, it is plausible that these compounds occupy the same subsites and that the production of compound **3** is increased by the mutation N216W and the unveiling of subsite +2'' (Fig. 7). However, considering the experimental and *in silico* data, it is likely that the linkage of *p*NP and its orientational constraints in compound **3** leads to less favorable interactions in subsite +2'', in particular with respect to residue Trp216 compared to compound **2** (parallel π-π stacking in Fig. 6D and H).

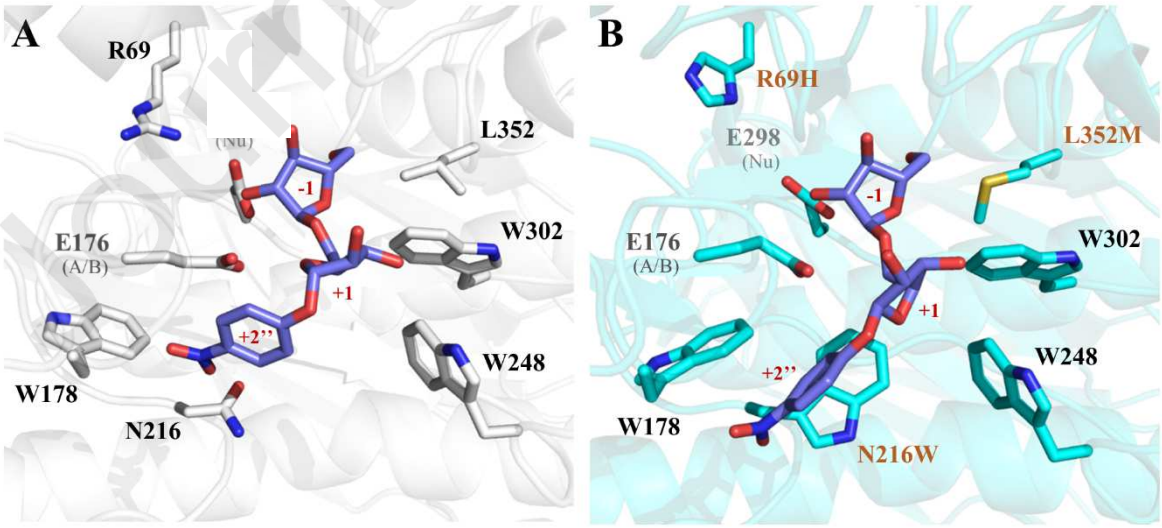

Fig. 7. Enzymes bound to the (1,5)-linked product **3**: (A**)** wild-type *Tx*Abf and (B) R69H-N216W-L352M. The protein is shown in cartoon, whereas the key labelled residues and the

ligands are shown in stick representation. Mutation and subsites are labelled (brown and red characters respectively).

4. Discussion

The α-L-arabinofuranosidase, *Tx*Abf is probably the best studied member of GH51, especially regarding its ability to perform glycosynthesis [33,34,45–48,58,59]. So far, we have shown that this enzyme possesses a wide range of capabilities, including the ability to synthesize D-galactofuranosides and is relatively amenable to enzyme engineering [33]. In the present study, we have revisited some of the more fundamental features of *Tx*Abf, in particular its ability to catalyze self-condensation reactions using either pento- or hexo-furanosides, focusing on the way in which mutagenesis of key residues modifies this property.

4.1. Key factors favoring self-condensation

Both mutations F26L and L352M have been reported to enhance the ability of *Tx*Abf to perform transglycosylation [46–48,60]. Moreover, in the case of L352M, we have shown that modification of *Tx*Abf properties is due to quite complex long-range effects that affect both the negative and positive subsites, whereas F26L only affects subsite -1 [48]. Here, we reveal that neither of these mutations produce major effects on self-condensation when compared to the more determining effect of the double mutation R69H-N216W. Clearly, these latter mutations are responsible for the most overall improvements in self-condensation reported in this work and, in the case of N216W mutation, for the acquisition of enhanced aptitude to form (1,3)-linked furanobiosides and α-L-(1,5)-linked arabinofuranobiosides. It is noteworthy that mutation R69H alone does not enhance the self-condensation ability of β-D-Gal*f*O*p*NP compared to the wild type *Tx*Abf. Compared to α-L-Ara*f*O*p*NP, the global repositioning of β-D-Gal*f*O*p*NP within subsites -1 of wild-type *Tx*Abf and the R69H-mutated enzyme is caused by the presence of the extra hydroxymethyl moiety at *C*-5. However, in R69H disruption is further compounded by the presence of H69, which impacts the positioning of both catalytic residues [47,48]. However, regarding self-condensation these two factors clearly do not produce a positive additive effect.

*4.2. Improving self-condensation of β-D-Galf*O*pNP*

One of the aims of this work was to improve the ability of *Tx*Abf to synthesize D-galactofurano-oligosaccharides. In previous work, we have shown that it is extremely difficult to determine the K_M value for reactions containing β-D-Gal*f*O*p*NP, catalyzed by the wild-type enzyme [33,55,56]. Moreover, performing both STD-NMR and ITC failed to reveal any measurable interactions between *Tx*Abf and β-D-Gal*f*O*p*NP [55]. Therefore, it was extremely gratifying to observe that the double mutant R69H-N216W not only improves self-condensation of β-D-Gal*f*O*p*NP, but also provides the basis to measure a K_M value that is similar to that measured for the wild-type enzyme in the presence of α-L-Ara*f*O*p*NP. Since the constant K_M (= $[k_3 \cdot (k_{-1} + k_2)]/[k_1 \cdot (k_2 + k_3)]$) is composed of both an affinity component ($1/K_d = k_1/k_{-1}$) and constants related to both glycosylation (k_2) and deglycosylation (k_3) steps, it is difficult to further analyze this improvement [32,61]. However, considering that β-D-Gal*f*O*p*NP possesses a good leaving group, we postulate that improvements in self-condensation of this compound are in part due to improved substrate binding.

4.3. Insights related to secondary hydrolysis

Data related to the mutants investigated herein supply insight on how secondary hydrolysis of glycosynthetic products might be modulated. In the case of the synthesis of D-galactofuranosyl disaccharides, secondary hydrolysis is clearly reduced or even imperceptible. One reason for this might be suboptimal positioning of the scissile inter-glycosidic bond with respect to the catalytic residues. In this regard, comparison of the 3D models of *Tx*Abf enzymes bound to compounds **1**, **2**, **4** and **5** reveals that the oxygen atom of the scissile bond of the self-condensation products are similarly distant (1.7-2.0 Å) from protonated Glu176 (acid/base). Likewise, the anomeric carbon is similarly located at 3.0-3.4 Å from Glu298 (nucleophile) (Supplementary Fig. S8). Therefore, in the absence of visible differences between the self-condensation product/enzyme pairs, it is plausible that the scissile inter-glycosidic bond in the D-galactofuranosyl disaccharides is dynamically mis-orientated (*i.e.* during conformational preactivation [62,63]) for hydrolysis. This might be the result of the additional hydroxymethyl group at the *C*-5 position on the furanose ring bound in subsite -1 and/or enzyme mutations.

It is worth recalling that compared to R69H-N216W, the introduction of L352M or F26L reveals decreased secondary hydrolysis (v_{HII}) of product **2** (Supplementary Table S1). Similarly,

the synthesis rates of **2** are decreased, especially for F26L-containing triple-mutant, although exactly how this affects both self-condensation and secondary hydrolysis is unclear. However, modification of the internal volume of the pocket-like subsite -1 and/or the interactions with the donor substrate might modulate the behavior of the triple-mutants.

4.4. Introduction of a tryptophan at position 216 forms a new binding subsite

A key finding in this study is the emergence of new regioselectivity, yielding (1,3)-linked pentofurano- and hexofurano-disaccharides. The introduction of tryptophan at position 216 contributes to this, although as a standalone mutation N216W is insufficient to procure altered regioselectivity. Nevertheless, regarding N216W, introduction of a tryptophan provides the basis for a new π-π interaction between the planar indolyl ring and the *p*NP aglycon moiety. It is relevant that the introduction of tryptophan into other GHs has also produced changes in regioselectivity, either by forcing the repositioning of the glycoside acceptor [64], or by creating a favorable interaction with the acceptor or its linked aromatic moiety [65,66]. It is also noteworthy that in *Tx*Abf, unveiling of the new subsite +2'' does not interfere with the original subsite +2. This infers that it could be possible through further enzyme engineering to block the subsite +2 and thus obtain an enzyme that procures mainly (1,3)-linked pentofurano- and hexofurano-disaccharides, perh[illegible]vith small traces of (1,5)-linked compounds; or inversely for the synthesis of (1,2)-linke[illegible]iosides.

5. Conclusion

This study c[illegible]utes to our understanding of how *Tx*Abf catalyzes self-condensation of pento- and hexofur[illegible]nd provides new mutants that can be added to the growing toolbox of biocatalysts [illegible] for glycosynthesis. Self-condensation reactions remain under kinetic control, meaning that high yields can be obtained using higher substrate concentrations, and that regioselectivity can be quite efficiently modulated. Bearing this in mind, it should be possible in the very near future to define reactions catalyzed by mutated enzymes that will procure high yields of relatively pure (1,3)-linked regioisomers. Likewise, with the knowledge of how to enhance the formation of (1,3)-linked regioisomers, it should also be possible to repress their formation, while identifying ways to enhance the regioselective formation of (1,2) linkages.

Acknowledgments

NMR analyses were performed using facilities at MetaToul (Metabolomics & Fluxomics Facilities, Toulouse, France, www.metatoul.fr), which is part of the national infrastructure MetaboHUB (The French National infrastructure for metabolomics and fluxomics, www.metabohub.fr) and is supported by grants from the Région Midi-Pyrénées, the European Regional Development Fund, SICOVAL, IBiSa-France, CNRS, and INRAE.

Funding

The PhD fellowship of J. Zhao was supported by CSC (China Scholarship Council).

Declaration of Competing Interest

The authors declare no conflict of interest.

Author contributions

R.F. and M.J.O designed and supervised the study. J.Z. performed the biochemical experiment. J.Z., J.E. and I.A. performed the docking experiment. All authors analyzed data and contributed to write the manuscript.

AppendixA. Supplementarymaterial

Supplementary data to this article can be found online at .

References

[1] P. Peltier, R. Euzen, R. Daniellou, C. Nugier-Chauvin, V. Ferrières, Recent knowledge and innovations related to hexofuranosides: structure, synthesis and applications, Carbohydr. Res. 343 (2008) 1897–1923. https://doi.org/10.1016/j.carres.2008.02.010.

[2] I. Chlubnová, D. Filipp, V. Spiwok, H. Dvoráková, R. Daniellou, C. Nugier-Chauvin, B. Králová, V. Ferrières, Enzymatic synthesis of oligo-D-galactofuranosides and L-arabinofuranosides: from molecular dynamics to immunological assays., Org. Biomol. Chem. 8 (2010) 2092–2102. https://doi.org/10.1039/b926988f.

[3] L.L. Pedersen, S.J. Turco, Galactofuranose metabolism: a potential target for antimicrobial chemotherapy, Cell. Mol. Life Sci. 60 (2003) 259–266.

https://doi.org/10.1007/s000180300021.

[4] J.B. Houseknecht, T.L. Lowary, Chemistry and biology of arabinofuranosyl- and galactofuranosyl-containing polysaccharides, Curr. Opin. Chem. Biol. 5 (2001) 677–682. https://doi.org/10.1016/S1367-5931(01)00265-4.

[5] H. Gruppen, R.A. Hoffmann, F.J.M. Kormelink, A.G.J. Voragen, J.P. Kamerling, J.F.G. Vliegenthart, Characterisation by ^{1}H NMR spectroscopy of enzymically derived oligosaccharides from alkali-extractable wheat-flour arabinoxylan, Carbohydr. Res. 233 (1992) 45–64. https://doi.org/10.1016/S0008-6215(00)90919-4.

[6] B. Seiboth, B. Metz, Fungal arabinan and L-arabinose metabolism, Appl. Microbiol. Biotechnol. 89 (2011) 1665–1673. https://doi.org/10.1007/s00253-010-3071-8.

[7] B. Classen, A. Baumann, J. Utermoehlen, Arabinogalactan-proteins in spore-producing land plants, Carbohydr. Polym. 210 (2019) 215–224. https://doi.org/10.1016/j.carbpol.2019.01.077.

[8] Y. Kawabata, S. Kaneko, I. Kusakabe, Y. Gama, Synthesis of regioisomeric methyl α-L-arabinofuranobiosides, Carbohydr. Res. 267 (1995) 39–47. https://doi.org/10.1016/0008-6215(94)00290-V.

[9] J.P. Joseleau, G. Chambat, M. Vignon, F. Barnoud, Chemical and ^{13}C N.M.R. studies on two arabinans from the inner bark of young stems of *Rosa glauca*, Carbohydr. Res. 58 (1977) 165–175. https://doi.org/10.1016/S0008-6215(00)83412-6.

[10] C. Marino, L. Baldoni, Synthesis of D-galactofuranose-containing molecules: design of galactofuranosyl acceptors, ChemBioChem. 15 (2014) 188–204. https://doi.org/10.1002/cbic.201300638.

[11] T.L. Lowary, Synthesis and conformational analysis of arabinofuranosides, galactofuranosides and fructofuranosides, Curr. Opin. Chem. Biol. 7 (2003) 749–756. https://doi.org/10.1016/j.cbpa.2003.10.005.

[12] C. Jones, A.R. Todeschini, A. Agrellos, J.O. Previato, L. Mendonça-Previato, Heterogeneity in the biosynthesis of mucin *O*-glycans from *Trypanosoma cruzi* Tulahuen strain with the expression of novel galactofuranosyl-containing oligosaccharides, Biochemistry. 43 (2004) 11889–11897. https://doi.org/10.1021/bi048942u.

[13] J.A. Leal, R. Gómez-Miranda, A. Prieto, J. Domenech, O. Ahrazem, M. Bernabé, Possible chemotypes from cell wall polysaccharides, as an aid in the systematics of *Penicillium* and its teleomorphic states *Eupenicillium* and *Talaromyces*, Mycol. Res. 101 (1997) 1259–1264. https://doi.org/10.1017/S0953756297004012.

[14] A. Prieto, M. Bernabé, J.A. Leal, Isolation, purification and chemical characterization of alkali-extractable polysaccharides from the cell walls of *Talaromyces* species, Mycol. Res. 99 (1995) 69–75. https://doi.org/10.1016/S0953-7562(09)80318-3.

[15] E.A. Leitão, V.C.B. Bittencourt, R.M.T. Haido, A.P. Valente, J. Peter-Katalinic, M. Letzel, L.M. de Souza, E. Barreto-Bergter, β-Galactofuranose-containing *O*-linked oligosaccharides present in the cell wall peptidogalactomannan of *Aspergillus fumigatus* contain immunodominant epitopes, Glycobiology. 13 (2003) 681–692. https://doi.org/10.1093/glycob/cwg089.

[16] U. Sørum, B. Robertsen, L. Kenne, Structural studies of the major polysaccharide in the cell wall of *Renibacterium salmoninarum*, Carbohydr. Res. 306 (1998). https://doi.org/10.1016/S0008-6215(97)10071-4.

[17] A. Trincone, Uncommon glycosidases for the enzymatic preparation of glycosides, Biomolecules. 5 (2015) 2160–2183. https://doi.org/10.3390/biom5042160.

[18] C. Marino, A. Rinflerch, R.M. De Lederkremer, Galactofuranose antigens, a target for diagnosis of fungal infections in humans, Futur. Sci. OA. 3 (2017) FSO199. https://doi.org/10.4155/fsoa-2017-0030.

[19] T. Konishi, H. Ono, M. Ohnishi-Kameyama, S. Kaneko, T. Ishii, Identification of a mung bean arabinofuranosyltransferase that transfers arabinofuranosyl residues onto (1,5)-linked α-L-arabino-oligosaccharides, Plant Physiol. 141 (2006) 1098–1105. https://doi.org/10.1104/pp.106.080309.

[20] N.L. Rose, G.C. Completo, S.J. Lin, M. McNeil, M.M. Palcic, T.L. Lowary, Expression, purification, and characterization of a galactofuranosyltransferase involved in *Mycobacterium tuberculosis* arabinogalactan biosynthesis, J. Am. Chem. Soc. 128 (2006) 6721–6729. https://doi.org/10.1021/ja058254d.

[21] M. Belanova, P. Dianiskova, P.J. Brennan, G.C. Completo, N.L. Rose, T.L. Lowary, K. Mikusova, Galactosyl transferases in mycobacterial cell wall synthesis, J. Bacteriol. 190 (2008) 1141–1145. https://doi.org/10.1128/JB.01326-07.

[22] A. Castilho, G. Beihammer, C. Pfeiffer, K. Göritzer, L. Montero-Morales, U. Vavra, D. Maresch, C. Grünwald-Gruber, F. Altmann, H. Steinkellner, R. Strasser, An oligosaccharyltransferase from *Leishmania major* increases the *N*-glycan occupancy on recombinant glycoproteins produced in *Nicotiana benthamiana*, Plant Biotechnol. J. 16 (2018) 1700–1709. https://doi.org/10.1111/pbi.12906.

[23] S. Kallolimath, C. Gruber, H. Steinkellner, A. Castilho, Promoter choice impacts the efficiency of plant glyco-engineering, Biotechnol. J. 13 (2018) 1700380. https://doi.org/10.1002/biot.201700380.

[24] L. Montero-Morales, H. Steinkellner, Advanced plant-based glycan engineering, Front. Bioeng. Biotechnol. 9 (2018) 81. https://doi.org/10.3389/fbioe.2018.00081.

[25] B. Nidetzky, A. Gutmann, C. Zhong, Leloir glycosyltransferases as biocatalysts for chemical production, ACS Catal. 8 (2018) 6283–6300. https://doi.org/10.1021/acscatal.8b00710.

[26] M.R. Richards, T.L. Lowary, Chemistry and biology of galactofuranose-containing polysaccharides, ChemBioChem. 10 (2009) 1920–1938. https://doi.org/10.1002/cbic.200900208.

[27] J. Houseknecht, T.L. Lowary, Oligofuranosides containing conformationally restricted residues: synthesis and conformational analysis, J. Org. Chem. 67 (2002) 4064. https://doi.org/10.1021/jo011127p.

[28] H.A. Taha, M.R. Richards, T.L. Lowary, Conformational analysis of furanoside-containing mono- and oligosaccharides, Chem. Rev. 113 (2013) 1851–1876. https://doi.org/10.1021/cr300249c.

[29] D.E. Koshland, Stereochemistry and the mechanism of enzymatic reactions, Biol. Rev. 28 (1953) 416–436. https://doi.org/10.1111/j.1469-185X.1953.tb01386.x.

[30] S.A. Barker, E.J. Bourne, M. Stacey, R.B. Ward, Some paper-chromatographic studies with *Aspergillus niger* '152' transfructosylase, Biochem. J. 69 (1958) 60–62. https://doi.org/10.1042/bj0690060.

[31] Y.K. Park, M.M. Almeida, Production of fructooligosaccharides from sucrose by a

transfructosylase from *Aspergillus niger*, World J. Microbiol. Biotechnol. 7 (1991) 331–334. https://doi.org/10.1007/BF00329399.

[32] B. Bissaro, P. Monsan, R. Fauré, M.J. O'Donohue, Glycosynthesis in a waterworld: new insight into the molecular basis of transglycosylation in retaining glycoside hydrolases, Biochem. J. 467 (2015) 17–35. https://doi.org/10.1042/BJ20141412.

[33] C. Rémond, R. Plantier-Royon, N. Aubrya, M.J. O'Donohue, An original chemoenzymatic route for the synthesis of β-D-galactofuranosides using an α-L-arabinofuranosidase, Carbohydr. Res. 340 (2005) 637–644. https://doi.org/10.1016/j.carres.2005.01.016.

[34] C. Rémond, R. Plantier-Royon, N. Aubry, E. Maes, C. Bliard, M.J. O'Donohue, Synthesis of pentose-containing disaccharides using a thermostable α-L-arabinofuranosidase, Carbohydr. Res. 339 (2004) 2019–2025. https://doi.org/10.1016/j.carres.2004.04.017.

[35] I. Chlubnová, B. Králová, H. Dvořáková, P. Hošek, V. Spiwok, D[illegible], C. Nugier-Chauvin, R. Daniellou, V. Ferrières, The versatile enzyme Ara51 allowed efficient synthesis of rare pathogen-related β-D-galactofuranosyl-pyranoside disaccharides, Org. Biomol. Chem. 12 (2014) 3080–3089. https://doi.or[illegible]1039/c3ob42519c.

[36] I. Chlubnová, B. Králová, H. Dvořáková, V. Spiwo[illegible]ipp, C. Nugier-Chauvin, R. Daniellou, V. Ferrières, Biocatalyzed synthesis o[illegible]osides and their ability to trigger production of TNF-α, Bioorg. Med. Ch[illegible]t. 26 (2016) 1550–1553. https://doi.org/10.1016/j.bmcl.2016.02.018.

[37] V. Lombard, H. Golaconda Ramulu, E. Drula, P.M. Coutinho, B. Henrissat, The carbohydrate-active enzymes database (CAZy) in 2013, Nucleic Acids Res. 42 (2014) D490–D495. https://doi.org/10.1093/nar/gkt1178.

[38] M. Seničar, L. Legentil, V. Ferrières, S. V. Eliseeva, S. Petoud, K. Takegawa, P. Lafite, R. Daniellou, Galactofuranosidase from JHA 19 *Streptomyces* sp.: subcloning and biochemical characterization, Carbohydr. Res. 480 (2019) 35–41. https://doi.org/10.1016/j.carres.2019.05.011.

[39] M. Seničar, P. Lafite, S. V. Eliseeva, S. Petoud, L. Landemarre, R. Daniellou, Galactofuranose-related enzymes: challenges and hopes, Int. J. Mol. Sci. 21 (2020) 3465. https://doi.org/10.3390/ijms21103465.

[40] W. Helbert, L. Poulet, S. Drouillard, S. Mathieu, M. Loiodice, M. Couturier, V. Lombard, N. Terrapon, J. Turchetto, R. Vincentelli, B. Henrissat, Discovery of novel carbohydrate-active enzymes through the rational exploration of the protein sequences space, Proc. Natl. Acad. Sci. U.S.A. 116 (2019) 6063–6068. https://doi.org/10.1073/pnas.1815791116.

[41] E. Matsunaga, Y. Higuchi, K. Mori, N. Yairo, T. Oka, S. Shinozuka, K. Tashiro, M. Izumi, S. Kuhara, K. Takegawa, Identification and characterization of a novel galactofuranose-specific β-D-galactofuranosidase from *Streptomyces* species, PLoS ONE. 10 (2015) e0137230. https://doi.org/10.1371/journal.pone.0137230.

[42] E. Matsunaga, Y. Higuchi, K. Mori, N. Yairo, S. Toyota, T. Oka, K. Tashiro, K. Takegawa, Characterization of a PA14 domain-containing galactofuranose-specific β-D-galactofuranosidase from *Streptomyces* sp., Biosci. Biotechnol. Biochem. 81 (2017) 1314–1319. https://doi.org/10.1080/09168451.2017.1300518.

[43] T. Debeche, N. Cummings, I. Connerton, P. Debeire, M.J. O'Donohue, Genetic and

biochemical characterization of a highly thermostable α-L-arabinofuranosidase from *Thermobacillus xylanilyticus*, Appl. Environ. Microbiol. 66 (2000) 1734–1736. https://doi.org/10.1128/AEM.66.4.1734-1736.2000.

[44] T. Debeche, C. Bliard, P. Debeire, M.J. O'Donohue, Probing the catalytically essential residues of the α-L-arabinofuranosidase from *Thermobacillus xylanilyticus*, Protein Eng. Des. Sel. 15 (2002) 21–28. https://doi.org/10.1093/protein/15.1.21.

[45] F. Arab-Jaziri, B. Bissaro, C. Tellier, M. Dion, R. Fauré, M.J. O'Donohue, Enhancing the chemoenzymatic synthesis of arabinosylated xylo-oligosaccharides by GH51 α-L-arabinofuranosidase, Carbohydr. Res. 401 (2015) 64–72. https://doi.org/10.1016/j.carres.2014.10.029.

[46] F. Arab-Jaziri, B. Bissaro, M. Dion, O. Saurel, D. Harrison, F. Ferreira, A. Milon, C. Tellier, R. Fauré, M.J. O'Donohue, Engineering transglycosidase activity into a GH51 α-L-arabinofuranosidase, New Biotechnol. 30 (2013) 536–544. https://doi.org/10.1016/j.nbt.2013.04.002.

[47] B. Bissaro, J. Durand, A. Planas, P. Monsan, X. Biarnés, A. Planas, P. Monsan, M.J. O'Donohue, R. Fauré, Molecular design of non-Leloir xylose-transferring enzymes from an α-L-arabinofuranosidase: a rationale for the engineering of evolved transglycosylases, ACS Catal. 5 (2015) 4598–4611. https://doi.org/10.1021/acscatal.5b00949.

[48] J. Zhao, T. Tandrup, B. Bissaro, S. Barbe, J.-C.N. Poulsen, I. André, C. Dumon, L. Lo Leggio, M.J. O'Donohue, R. Fauré, Probing the determinants of the transglycosylation/hydrolysis partition in a retaining α-L-arabinofuranosidase, New Biotechnol. 62 (2021) 68–78. https://doi.org/10.1016/j.nbt.2021.01.008.

[49] P.K. Glasoe, F.A. Long, Use of glass electrodes to measure acidities in deuterium oxide, J. Phys. Chem. 64 (1960) 188–190. https://doi.org/10.1021/j100830a521.

[50] H.E. Gottlieb, V. Kotlyar, A. Nudelman, NMR chemical shifts of common laboratory solvents as trace impurities, J. Org. Chem. 62 (1997) 7512–7515. https://doi.org/10.1021/jo971176v.

[51] D.A. Case, R.M. Betz, D.S. Cerutti, T.E. Cheatham III, T.A. Darden, R.E. Duke, T.J. Giese, H. Gohlke, A.W. Goetz, N. Homeyer, S. Izadi, P. Janowski, J. Kaus, A. Kovalenko, T.S. Lee, S. LeGrand, P. Li, C. Lin, T. Luchko, R. Luo, B. Madej, D. Mermelstein, K.M. Merz, G. Monard, H. Nguyen, H.T. Nguyen, I. Omelyan, A. Onufriev, D.R. Roe, A. Roitberg, C. Sagui, C.L. Simmerling, W.M. Botello-Smith, J. Swails, R.C. Walker, J. Wang, R.M. Wolf, X. Wu, L. Xiao, P.A. Kollman, AMBER 2016, University of California, San Francisco (2016). https://ambermd.org/doc12/Amber16.pdf

[52] M.D. Hanwell, D.E. Curtis, D.C. Lonie, T. Vandermeersch, E. Zurek, G.R. Hutchison, Avogadro: an advanced semantic chemical editor, visualization, and analysis platform, J. Cheminform. 4 (2012) 17. https://doi.org/10.1186/1758-2946-4-17.

[53] The PyMOL molecular graphics system, Version 1.8 Schrödinger, LLC. https://pymol.org/2/support.html

[54] E. Krieger, G. Vriend, YASARA view -molecular graphics for all devices- from smartphones to workstations, Bioinformatics 30 (2014) 2981–2982. https://doi.org/10.1093/bioinformatics/btu426.

[55] F. Arab-Jaziri, B. Bissaro, S. Barbe, O. Saurel, H. Débat, C. Dumon, V. Gervais, A. Milon, I. André, R. Fauré, M.J. O'Donohue, Functional roles of H98 and W99 and β2α2

loop dynamics in the α-L-arabinofuranosidase from *Thermobacillus xylanilyticus*, FEBS J. 279 (2012) 3598–3611. https://doi.org/10.1111/j.1742-4658.2012.08720.x.

[56] R. Euzen, G. Lopez, C. Nugier-Chauvin, V. Ferrières, D. Plusquellec, C. Rémond, M. O'Donohue, A chemoenzymatic approach for the synthesis of unnatural disaccharides containing D-galacto- or D-fucofuranosides, Eur. J. Org. Chem. (2005) 4860–4869. https://doi.org/10.1002/ejoc.200500525.

[57] G. Paës, L.K. Skov, M.J. O'Donohue, C. Rémond, J.S. Kastrup, M. Gajhede, O. Mirza, The structure of the complex between a branched pentasaccharide and *Thermobacillus xylanilyticus* GH-51 arabinofuranosidase reveals xylan-binding determinants and induced fit, Biochemistry. 47 (2008) 7441–51. https://doi.org/10.1021/bi800424e.

[58] C. Rémond, M. Ferchichi, N. Aubry, R. Plantier-Royon, C. Portella, M.J. O'Donohue, Enzymatic synthesis of alkyl arabinofuranosides using a thermostable α-L-arabinofuranosidase, Tetrahedron Lett. 43 (2002) 9653–9655. https://doi.org/10.1016/S0040-4039(02)02381-X.

[59] B. Bissaro, O. Saurel, F. Arab-jaziri, L. Saulnier, A. Milon, M. Tenkanen, P. Monsan, M.J. O'Donohue, R. Fauré, Mutation of a pH-modulating residue in a GH51 α-L-arabinofuranosidase leads to a severe reduction of the secondary hydrolysis of transfuranosylation products, Biochim. Biophys. Acta - Subj. 1840 (2014) 626–636. https://doi.org/10.1016/j.bbagen.2013.10.013.

[60] D. Teze, J. Zhao, M. Wiemann, Z.G.A. Kazi, R. Lund, J. Leuner, M. Vuillemin, M.E. Rønne, G. Carlström, J.Ø. Duus, Y.-H. Sanejouand, M.J. O'Donohue, E. Nordberg Karlsson, R. Fauré, H. Stålbrand, B. Svensson, Rational enzyme design without structural knowledge: a sequence-based approach for efficient generation of transglycosylases, Chem. Eur. J. 27 (2021) 10323–10334. https://doi.org/10.1002/chem.202100110.

[61] K.A. Johnson, A century of enzyme kinetic analysis, 1913 to 2013, FEBS Lett. 587 (2013) 2753–2766. https://doi.org/10.1016/j.febslet.2013.07.012.

[62] N. G. S. McGregor, M. A. Nin-Hill, D. Linzel, M. Haon, J. Reijngoud, A. Ram, M.-N. Rosso, G. A. van der Marel, J. D. C. Codée, G. P. van Wezel, J.-G. Berrin, C. Rovira, H. S. Overkleeft, G. J. Davies, Rational design of mechanism-based inhibitors and activity-based probes for the identification of retaining α-L-arabinofuranosidases, J. Am. Chem. Soc. 142 (2020) 4648–4662. https://doi.org/10.1021/jacs.9b11351.

[63] K. Hövel, D. Shallom, K. Niefind, V. Belakhov, G. Shoham, T. Baasov, Y. Shoham, D. Schomburg, Crystal structure and snapshots along the reaction pathway of a family 51 α-L-arabinofuranosidase, EMBO J. 22 (2003) 4922–4932. https://doi.org/10.1093/emboj/cdg494.

[64] V. Tran, L. Hoffmann, C. Rabiller, C. Tellier, M. Dion, Rational design of a GH1 β-glycosidase to prevent self-condensation during the transglycosylation reaction, Protein Eng. Des. Sel. 23 (2010) 43–49. https://doi.org/10.1093/protein/gzp068.

[65] J. Madhuprakash, A. Singh, S. Kumar, M. Sinha, P. Kaur, S. Sharma, A.R. Podile, T.P. Singh, Structure of chitinase D from *Serratia proteamaculans* reveals the structural basis of its dual action of hydrolysis and transglycosylation, Int. J. Biochem. Mol. Biol. 4 (2013) 166–178.

[66] A. Rosengren, S.K. Reddy, J.S. Sjöberg, O. Aurelius, D.T. Logan, K. Kolenová, H. Stålbrand, An *Aspergillus nidulans* β-mannanase with high transglycosylation capacity

792 revealed through comparative studies within glycosidase family 5, Appl. Microbiol.
793 Biotechnol. 98 (2014) 10091–10104. https://doi.org/10.1007/s00253-014-5871-8.

794

795

796